Quantum phase transition in a Heisenberg antiferromagnet on a square lattice with strong plaquette interactions

A. Fabricio Albuquerque,[1] Matthias Troyer,[2] and Jaan Oitmaa[1]

[1]*School of Physics, The University of New South Wales, Sydney, New South Wales 2052, Australia*

[2]*Theoretische Physik, ETH Zurich, 8093 Zurich, Switzerland*

We present numerical results for an $S=1/2$ Heisenberg antiferromagnet on an inhomogeneous square lattice with tunable interaction between spins belonging to different plaquettes. Employing quantum Monte Carlo, we significantly improve on previous results for the critical point separating singlet-disordered and Néel-ordered phases and obtain an estimate for the critical exponent ν consistent with the three-dimensional classical Heisenberg universality class. Additionally, we show that a fairly accurate result for the critical point can be obtained from a contractor renormalization expansion by applying a surprisingly simple analysis to the effective Hamiltonian.

PACS number(s): 75.10.Jm, 02.70.Ss, 75.40.Mg

I. INTRODUCTION

The square lattice quantum Heisenberg antiferromagnet (SLQHA) with spin $S=1/2$ is one of the paradigmatic models in condensed-matter physics and has been extensively investigated in the last two decades, mainly in connection with the parent compounds of cuprate superconductors.[1] Good agreement with experimental data is obtained from the analysis of an effective continuous field theory rigorously justified in the limit of large spin S given by the $(2+1)$-dimensional nonlinear σ model (NLσM).[2] The coupling g in the NLσM controls the transition between Néel-ordered and quantum-disordered phases and it can be shown that the SLQHA maps to the renormalized classical regime of the NLσM ($g < g_c$), which therefore has a long-range-ordered ground state.[1,2]

The proximity to a quantum critical point may, however, lead to a crossover to a finite temperature quantum critical regime where thermodynamic quantities are affected by strong quantum fluctuations and display universal behavior.[2,3] Nevertheless, numerical simulations[4] indicate that this crossover may be too narrow to be detectable possibly due to the fact that the SLQHA is deep inside the renormalized classical regime. This difficulty has motivated the investigation of antiferromagnets defined on *decorated* square lattices where the proximity to a quantum critical point separating singlet-disordered and Néel-ordered phases is controlled by adjusting couplings in the Hamiltonian.[5–10]

We consider an $S=1/2$ Heisenberg Hamiltonian defined on the "plaquettized" square lattice depicted in Fig. 1,

$$\mathcal{H} = J\sum_{\langle i,j\rangle} \vec{S}_i \cdot \vec{S}_j + J'\sum_{\langle i,j\rangle'} \vec{S}_i \cdot \vec{S}_j. \tag{1}$$

J ($\langle i,j\rangle$, bold lines in Fig. 1) and J' ($\langle i,j\rangle'$, thin lines in Fig. 1) are, respectively, intraplaquette and interplaquette nearest-neighbor antiferromagnetic interactions. Since the model is self-dual under the transformation $J \leftrightarrow J'$, we apply the restriction $J' \leq J$ without losing generality and set $J=1$. Similarly to what happens with the aforementioned models with tunable interactions,[5–10] the ratio J'/J (equivalent to g^{-1} in the NLσM) controls the magnitude of quantum fluctuations

and a quantum phase transition at J'_C/J belonging to the universality class of the three-dimensional (3D) classical Heisenberg model[2] separates a disordered singlet phase at low J'/J from the renormalized classical state at $J'/J=1$, where the original SLQHA is recovered. Previous results for this "plaquettized" Heisenberg antiferromagnet were obtained analytically,[11] from series expansions,[11,12] exact diagonalization of small clusters,[13,14] and by diagonalizing the effective model obtained from a contractor renormalization (CORE) expansion.[15,16] The currently best estimate for the critical point [$J'_C/J=0.555(10)$] was obtained from an Ising series expansion.[12]

We investigate the model defined by Eq. (1) by means of quantum Monte Carlo (QMC) simulations and CORE with a twofold purpose. First, we would like to improve on previous estimates[11–16] for the quantum critical point. This might pave the way to future investigations of, for instance, the effects of impurities in a quantum critical antiferromagnet.[17–19] Second, we are interested in testing the quality of the results obtained from a CORE expansion including longer-ranged effective interactions than in Refs. 15 and 16 and by applying a simpler analysis to the effective Hamiltonian.
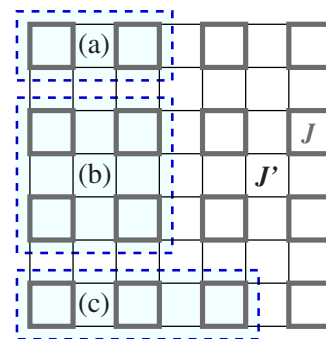

FIG. 1. (Color online) The "plaquettized" square lattice considered in this Brief Report: nearest-neighbor spins lying on the same (neighboring) plaquette(s) interact via superexchange J (J') represented by thick (thin) continuous lines [see Eq. (1)]. Dashed lines highlight the clusters employed in obtaining the range-1 (a), -2$^{1/2}$ (b), and −2 (c) CORE results.

II. NUMERICAL RESULTS

A. Quantum Monte Carlo

We have performed QMC simulations for the model described by Eq. (1) by employing the ALPS (Algorithms and Libraries for Physics Simulations) libraries'[20] implementation of the *directed loops* algorithm[21,22] for the stochastic series expansion (SSE) representation.[23] Lattices with $L \times L$ sites ($L/2 \times L/2$ plaquettes) with L up to 36 have been considered with periodic boundary conditions along both directions. Temperatures are set so as to ensure that ground-state properties are accessed: For each system's size, simulations were performed for inverse temperatures $\beta_n = 2^n$ so that the obtained averages agreed (within error bars) for β_n and β_{n-1}.[24] We have calculated the spin stiffness ρ_S and the second-order Binder cumulant for the staggered magnetization Q_2. The spin stiffness is obtained in terms of the winding numbers w_x and w_y,

$$\rho_S = \frac{1}{2\beta L^2}\langle w_x^2 + w_y^2 \rangle, \qquad (2)$$

and is expected to scale close to the critical point like $\rho_S \sim L^{2-d-z}$, where $d=2$ is the dimensionality and the dynamic critical exponent is expected to be $z=1$.[25] Therefore the quantity $\rho_S L$ should assume a size-independent value at the critical point, something confirmed by our results shown in Fig. 2(a). The second-order Binder cumulant for the staggered magnetization (m_s^z) is defined as

$$Q_2 = \frac{\langle (m_s^z)^4 \rangle}{\langle (m_s^z)^2 \rangle^2}. \qquad (3)$$

Q_2 also displays universal behavior in the critical regime and curves for different lattice sizes cross close to the critical point (not shown).

In order to locate the quantum critical point J_C'/J, we first analyze the scaling behavior of the intersection points between curves for $\rho_S L$ and Q_2 obtained for lattice sizes $(L, 2L)$. Crossing points are determined by performing linear and quadratic fits to different data subsets and deviations between different estimates are used in setting (generous) error bars. The so-obtained results are plotted in Fig. 2(b) as a function of $1/L$. We remark that, similarly to what was found in Ref. 10 for dimerized magnets, fastest convergence to the thermodynamic limit is attained for $\rho_S L$ and therefore focus on the results for this quantity in what follows.[26] Since the curvature for the crossing points decreases with increasing L [Fig. 2(b)], an upper bound for J_C'/J is simply obtained by applying a linear extrapolation to the three largest $(L, 2L)$ crossing points; a lower bound is directly given by the crossing point for the largest pair $(L, 2L)$. In this way, we arrive at the result $J_C'/J = 0.5485(12)$.[26]

In trying to achieve higher accuracy and additionally estimate the critical exponent associated to the correlation length ν, we employ the scaling ansatz

$$\rho_S(t, L) = L^{-1} f_{\rho_S}(t L^{1/\nu}), \qquad (4)$$

with reduced coupling $t = (J' - J_C')/J_C'$. By plotting $\rho_S L$ versus $t L^{1/\nu}$ and adjusting the values of J_C'/J and ν, we achieve data
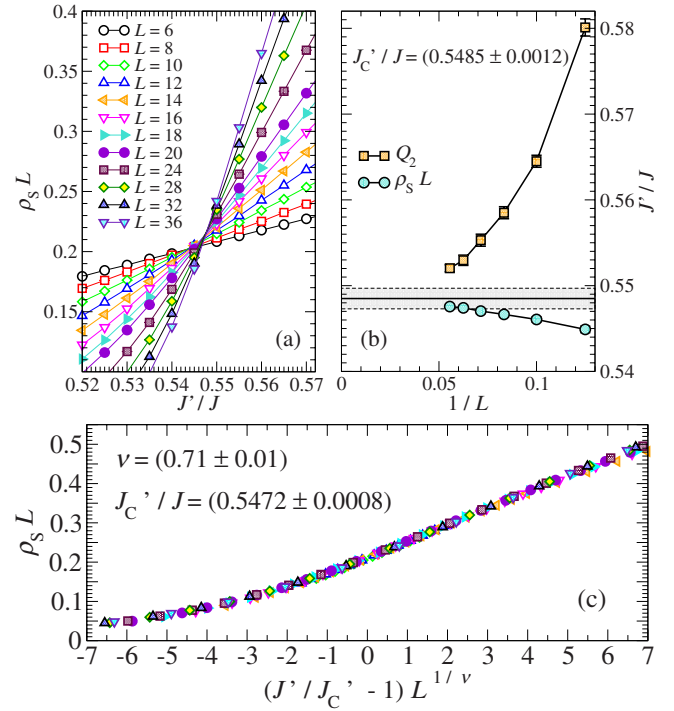

FIG. 2. (Color online) (a) SSE-QMC data for spin stiffness ρ_S multiplied by the system's size L as a function of the interplaquette coupling J'/J for temperatures $T \leq 1/2L$. Error bars are much smaller than the symbols' size. (b) Convergence of the intersection points for curves L and $2L$ for $\rho_S L$ [data shown in (a)] and second-order Binder cumulant Q_2 (not shown). Extrapolation (see main text) gives us the estimate $J_C'/J = 0.5485(12)$ for the critical point. (c) Data collapse for $\rho_S L$ is attained for $J_C'/J = 0.5472(8)$ and $\nu = 0.71(1)$ using the scaling ansatz of Eq. (4).

collapse for $J_C'/J = 0.5472(8)$ and $\nu = 0.71(1)$ as shown in Fig. 2(c).[26]

Our results for J_C'/J are consistent with earlier estimates[11–16] but improve on the previously best result $[J_C'/J = 0.555(10)$; Ref. 12] by one order of magnitude. Furthermore, our estimate for the critical exponent ν is compatible with the most accurate result for the 3D classical Heisenberg model $[\nu = 0.7112(5)$; Ref. 27] as expected from the mapping onto a NLσM.[2] Further improvements in the values for J_C'/J and ν may be achieved by simulating larger systems and/or applying a more sophisticated data analysis taking into account subleading finite-size corrections.[10,28]

B. Contractor renormalization

The CORE method[30,31] is a tool in deriving low-energy effective Hamiltonians for lattice models and was previously applied to the spin Hamiltonian on the modulated square lattice [Eq. (1)] by Capponi *et al.*[15,16] We extend their results by deriving a longer-ranged CORE expansion. We also notice that our CORE expansion is essentially a strong-coupling (on-site repulsion $U \to \infty$) version of the one derived in Ref. 32 where an effective Hamiltonian for the Hubbard model on the square lattice was obtained, but we have the advantages of a more natural motivation for choos-

ing the plaquettes as elementary blocks and of the absence of charge degrees of freedom.

We start by noticing that the original spin model described by Eq. (1) is particularly amenable to a CORE analysis, for the strongly coupled plaquettes are a natural choice as the elementary blocks (see Fig. 1; for details on the CORE procedure the reader is referred to Refs. 16 and 32). The retained low-lying block states are the plaquette's singlet ground state $|s\rangle$ and the triplet states $|t^\alpha\rangle$ with $\alpha=-1,0,+1$ denoting the total S^z component. This choice for the restricted local basis is justified by the fact that $|s\rangle$ and $|t^\alpha\rangle$ are the lowest block's eigenstates and also, as shown by Capponi *et al.*,[15,16] by their large weight in the density matrix of a plaquette embedded in a larger cluster. Effective couplings between these retained block states are obtained by subsequently diagonalizing a cluster comprised of connected plaquettes: A matching number of the cluster's low-lying eigenstates is projected upon the basis formed by the tensor products of local singlets and triplets, an effective Hamiltonian being obtained by imposing the constraint that the cluster's low-energy spectrum is exactly reproduced and by subtracting interactions previously obtained from clusters involving lesser plaquettes. We employ the clusters highlighted in Fig. 1 and label the results according to the longest range effective couplings obtained at each step of the CORE expansion: Range-1 interactions are obtained from the cluster comprised by two connected plaquettes depicted in Fig. 1(a), range-$2^{1/2}$ from a four-plaquette cluster [Fig. 1(b)], and range-2 from the cluster displaying three aligned plaquettes shown in Fig. 1(c).

The effective model resulting from the above procedure is expected to evidence dominant microscopic mechanisms at play in the original model and physically sound results are ideally obtained by means of a simplified subsequent analysis. We stress that our approach differs from the previous one[15,16] in a crucial way: While Capponi *et al.*[15,16] restricted their CORE expansion to the shortest range and studied the resulting range-1 effective Hamiltonian by means of exact diagonalizations, we expect that good results are obtainable in a simpler way from an extended CORE expansion including longer-ranged interactions. Accordingly, we locate the quantum critical point by determining the value of J'/J where the gap for triplet excitations (Δ) vanishes and estimate Δ from the effective CORE Hamiltonian simply as

$$\Delta = \mu_t - 4(t_1 + t_2 + t_3). \tag{5}$$

μ_t is the chemical potential for triplet excitations above the singlet ground state for low J'/J and the second term accounts for the triplons' kinetic energy: t_1 is the nearest-neighbor (NN), t_2 is the next-NN, and t_3 is the third-NN hopping amplitudes.[33] In other words, Eq. (5) is the energy of an *isolated* triplon in a *singlet sea*.

Results for $\Delta(J'/J)$ obtained from range-1, range-$2^{1/2}$, and range-2 CORE expansions are shown in Fig. 3 compared with the ones obtained from the plaquette series expansion derived in Ref. 12.[29] As expected, all results mutually agree in the limit of small J'/J where they are essentially exact; for larger J'/J, range-$2^{1/2}$ and range-2 CORE results underestimate Δ. However, the values of J'/J where range-$2^{1/2}$ and
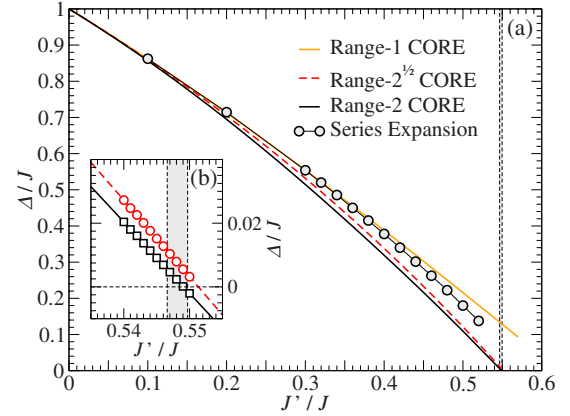

FIG. 3. (Color online) (a) Spin gap in the disordered phase of the spin model on the modulated square lattice described by Hamiltonian Eq. (1). Results have been obtained from a plaquette series expansion (Ref. 29) (circles; Ref. 12) and various range CORE analysis (see main text). The vertical dashed lines indicate values of J'/J consistent with the critical point obtained from QMC simulations ($J'_C/J \in [0.5466, 0.5497]$). The zoom in the inset (b) shows that values for the critical point consistent with the ones obtained from QMC are obtained from range-2 (squares) CORE results (range-$2^{1/2}$ results are represented by red circles).

range-2 results for Δ vanish are in surprisingly good agreement with the QMC results for J'_C/J presented in Sec. II A: $J'/J \approx 0.5513$ for range-$2^{1/2}$ and $J'/J \approx 0.5491$ for range-2. These values are seemingly converging very fast to a result consistent with the QMC estimates and this suggests that the procedure employed here might lead to more precise estimates for the critical point than the one employed in Refs. 15 and 16 where $J'_C/J=0.55(5)$ was obtained. We conjecture that this unexpected accuracy is related to level crossings observed close to the point where Δ vanishes. However, obviously we cannot discard the possibility that this remarkable agreement is coincidental and remark that poorer results are obtained for intermediate values of J'/J with the consequence that Δ from CORE does not follow a power law (as seen from a logarithmic plot, not shown). However, it is desirable to further test the procedure employed here by considering similar spin models.[5–10]

III. CONCLUSIONS

Summarizing, we have investigated an $S=1/2$ Heisenberg antiferromagnet on a "plaquettized" square lattice (Fig. 1) by means of QMC and CORE. Our results for the quantum critical point separating the gapped-singlet and Néel-ordered phases, $J'_C/J=0.5485(12)$ and $J'_C/J=0.5472(8)$, obtained from QMC simulations, substantially improve on previous estimates,[11–16] and the obtained critical exponent $\nu=0.71(1)$ is consistent with the tridimensional classical Heisenberg model universality class[27] as expected from the mapping to a NLσM.[2]

We also highlight the surprisingly good result for the critical point extracted from a simple analysis of range-$2^{1/2}$ and range-2 effective CORE Hamiltonians. However, it is not presently possible to exclude the possibility that the good

agreement with QMC is coincidental and it would be interesting to further test the procedure employed here. The fact that CORE is immune to the infamous *sign problem* opens interesting research possibilities, and fermionic systems on a geometry similar to the one considered here[34] may be investigated.

Note added. While preparing the manuscript and after finishing our simulations, we became aware of work by Wenzel *et al.*[35,36] in which dimerized and quadrumerized two-dimensional antiferromagnets are investigated by QMC. By employing a more sophisticated data analysis and simulating larger lattices, they obtain more precise estimates for the critical point for the model considered in the present work.

ACKNOWLEDGMENTS

[1] E. Manousakis, Rev. Mod. Phys. **63**, 1 (1991).

[2] S. Chakravarty, B. I. Halperin, and D. R. Nelson, Phys. Rev. B **39**, 2344 (1989).

[3] A. V. Chubukov, S. Sachdev, and J. Ye, Phys. Rev. B **49**, 11919 (1994).

[4] J. K. Kim and M. Troyer, Phys. Rev. Lett. **80**, 2705 (1998).

[5] A. W. Sandvik and D. J. Scalapino, Phys. Rev. Lett. **72**, 2777 (1994).

[6] M. Troyer, H. Kontani, and K. Ueda, Phys. Rev. Lett. **76**, 3822 (1996).

[7] V. N. Kotov, O. Sushkov, Zheng Weihong, and J. Oitmaa, Phys. Rev. Lett. **80**, 5790 (1998).

[8] P. V. Shevchenko, A. W. Sandvik, and O. P. Sushkov, Phys. Rev. B **61**, 3475 (2000).

[9] M. Matsumoto, C. Yasuda, S. Todo, and H. Takayama, Phys. Rev. B **65**, 014407 (2001).

[10] L. Wang, K. S. D. Beach, and A. W. Sandvik, Phys. Rev. B **73**, 014431 (2006).

[11] A. Koga, S. Kumada, and N. Kawakami, J. Phys. Soc. Jpn. **68**, 642 (1999).

[12] R. R. P. Singh, Z. Weihong, C. J. Hamer, and J. Oitmaa, Phys. Rev. B **60**, 7278 (1999).

[13] A. Läuchli, S. Wessel, and M. Sigrist, Phys. Rev. B **66**, 014401 (2002).

[14] A. Voigt, Comput. Phys. Commun. **146**, 125 (2002).

[15] S. Capponi, A. Läuchli, and M. Mambrini, Phys. Rev. B **70**, 104424 (2004).

[16] S. Capponi, Theor. Chem. Acc. **116**, 524 (2006).

[17] S. Sachdev, C. Buragohain, and M. Vojta, Science **286**, 2479 (1999).

[18] K. H. Höglund, A. W. Sandvik, and S. Sachdev, Phys. Rev. Lett. **98**, 087203 (2007).

[19] K. H. Höglund and A. W. Sandvik, Phys. Rev. Lett. **99**, 027205 (2007).

[20] A. F. Albuquerque *et al.*, J. Magn. Magn. Mater. **310**, 1187 (2007).

[21] O. F. Syljuåsen and A. W. Sandvik, Phys. Rev. E **66**, 046701 (2002).

[22] F. Alet, S. Wessel, and M. Troyer, Phys. Rev. E **71**, 036706 (2005).

[23] A. W. Sandvik, Phys. Rev. B **59**, R14157 (1999).

[24] Convergence was tested for values of J'/J close to the critical point, as estimated from preliminary QMC runs.

[25] M. P. A. Fisher, P. B. Weichman, G. Grinstein, and D. S. Fisher, Phys. Rev. B **40**, 546 (1989).

[26] Results obtained from the analysis of the Binder cumulant, $J'_C/J=0.552(4)$ and $\nu=0.75(5)$, are consistent with the ones obtained from $\rho_S L$ but are less precise, seemingly due to stronger subleading finite-size corrections.

[27] M. Campostrini, M. Hasenbusch, A. Pelissetto, P. Rossi, and E. Vicari, Phys. Rev. B **65**, 144520 (2002).

[28] K. S. D. Beach, L. Wang, and A. W. Sandvik, arXiv:cond-mat/0505194 (unpublished).

[29] The series becomes inaccurate beyond the leftmost data point in Fig. 3.

[30] C. J. Morningstar and M. Weinstein, Phys. Rev. Lett. **73**, 1873 (1994).

[31] C. J. Morningstar and M. Weinstein, Phys. Rev. D **54**, 4131 (1996).

[32] E. Altman and A. Auerbach, Phys. Rev. B **65**, 104508 (2002).

[33] The actual expression for Δ, Eq. (5), changes according to the range of the CORE expansion: range-1 Δ is determined by μ_t and t_1 only, for range-$2^{1/2}$, t_2 is also included and for range-2 the full expression is recovered. At each step, corrections for μ_t and t_1 are taken into account.

[34] S. Trebst, U. Schollwöck, M. Troyer, and P. Zoller, Phys. Rev. Lett. **96**, 250402 (2006).

[35] S. Wenzel, L. Bogacz, and W. Janke, Phys. Rev. Lett. **101**, 127202 (2008).

[36] S. Wenzel and W. Janke, arXiv:0808.1418 (unpublished).